THE JOURNAL OF PHYSICAL CHEMISTRY Letters

Letter

pubs.acs.org/JPCL

Design of Two-Dimensional Graphene-like Dirac Materials β_{12}-$XBeB_5$ (X = H, F, Cl) from Non-graphene-like β_{12}-Borophene

Ji-Hui Yang,[†,§] Shiru Song,[‡,†,§] Shixuan Du,[*,‡] Hong-Jun Gao,[‡] and Boris I. Yakobson[*,†]

[†]Department of Materials Science and Nanoengineering, Rice University, Houston, Texas 77005, United States

[‡]Institute of Physics & University of Chinese Academy of Sciences, Chinese Academy of Science, Beijing 100190, China

Supporting Information

ABSTRACT: Two-dimensional (2D) Dirac materials and boron sheets have attracted intensive interest recently. However, 2D Dirac materials remain rare and difficult to be realized experimentally, and 2D boron sheets generally have high dynamical instability. Stimulated by the experimental observation of Dirac cones in nongraphene-like β_{12} boron sheets and based on the understanding of boron sheet electronic organization, we theoretically design new 2D Dirac materials β_{12}-$XBeB_5$ (X = H, F, Cl) with high stability. We confirm β_{12}-$HBeB_5$ as the global energy minimum among its 2D allotropes based on global structure search methods, a strong indication of its experimental feasibility. Our designed β_{12}-$HBeB_5$ has not only a high Fermi velocity, but also a Dirac state very robust against extraordinary large tensile strains, an advantage for flexible electronics applications. Our work opens a new avenue to designing feasible 2D Dirac materials and stabilizing borophene sheets.

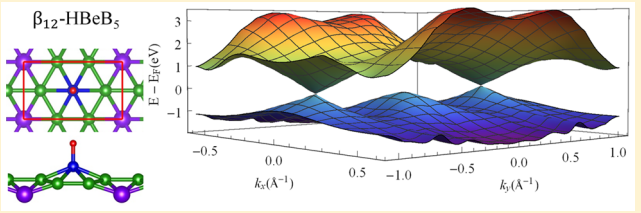

Ever since the discovery of graphene, many 2D materials have been extensively studied both experimentally and theoretically.[1−6] Among them, two-dimensional (2D) Dirac materials,[7] characterized by linear energy dispersion near the Fermi level, have shown potential for applications in next-generation nanoscale devices,[8] thanks to their unique electronic properties such as ballistic charge transport,[9] high carrier mobility,[10] and quantum Hall effect.[11] Despite the abundance of 2D materials, 2D Dirac materials are relatively rare due to the rigorous requirements on the symmetry, parameters, Fermi level, and band overlap in the materials to achieve Dirac cone features.[12] So far, only the Dirac state of graphene has been experimentally realized,[12] while the experimental feasibility and practical applications of the other theoretically predicted 2D Dirac materials such as S-, D-, and E-graphene[13] are still beyond reach. It is therefore important to identify, through experimental serendipity or sentient design, new 2D Dirac materials that are more likely to be realizable.

Among various potential systems, graphene-like boron sheet has attracted much interest as a good platform to design new 2D Dirac materials with fascinating properties. In graphene-like boron sheet, each boron atom has three valence electrons, and the Dirac states can be obtained by adding two electrons to each boron hexagonal ring. This can be achieved by embedding a metal atom of a suitable size, donating two electrons to the boron framework, as shown in Figure 1a. This strategy has been demonstrated in several systems like FeB_2,[14] TiB_2,[15] and strained BeB_2[16] monolayers. Similarly, as shown in Figure 1b, a triangular atomic layer of tetravalent metal like Mo sandwiched by two boron hexagonal layers can also form a Dirac state with double Dirac cones,[17] because each tetravalent metal atom can donate two electrons to each of the two boron hexagonal lattices. Additionally, the electron deficiency in boron leads to its novel bonding characters, i.e., boron can behave both covalently and ionically. Consequently, boron itself can also donate electrons to the hexagonal boron sheets and induce the Dirac states. For example, as shown in Figure 1c, in *P6/mmm* boron bilayers,[18] two boron hexagonal layers are vertically connected by B−B pairs. Each B−B pair has six valence electrons, two of which form a B−B covalent bond, leaving the other four electrons donated to the two boron hexagonal lattices and resulting in the double Dirac cone states. Similarly, in Figure 1d, *Pmmn*-boron can be seen as the boron chains attached above or below and parallel to the distorted graphene-like boron sheet.[19] In the chains, each boron atom forms two covalent-like bonds with two electrons left for each B−B pair. Then the B−B pair, which is ionic-like, donates the left two electrons to the distorted boron hexagonal lattices, resulting in the tilted Dirac state with ultrahigh and anisotropic carrier mobility.[20] Despite the great promise of those above systems in achieving Dirac states, the graphene-like boron sheet has not been realized yet due to its higher energy. Instead, recent theoretical and experimental works have demonstrated the realization of nongraphene-like 2D boron sheets composed of triangular and hexagonal boron motifs.[4,5,21−24] Some other boron sheets like M-boron, which is entirely composed of B_{20} clusters in a hexagonal arrangement with magnetic properties, are also predicted.[25] Straightforwardly, it would be more

Received: August 16, 2017
Accepted: September 8, 2017
Published: September 8, 2017

DOI: 10.1021/acs.jpclett.7b02163
J. Phys. Chem. Lett. 2017, 8, 4594−4599

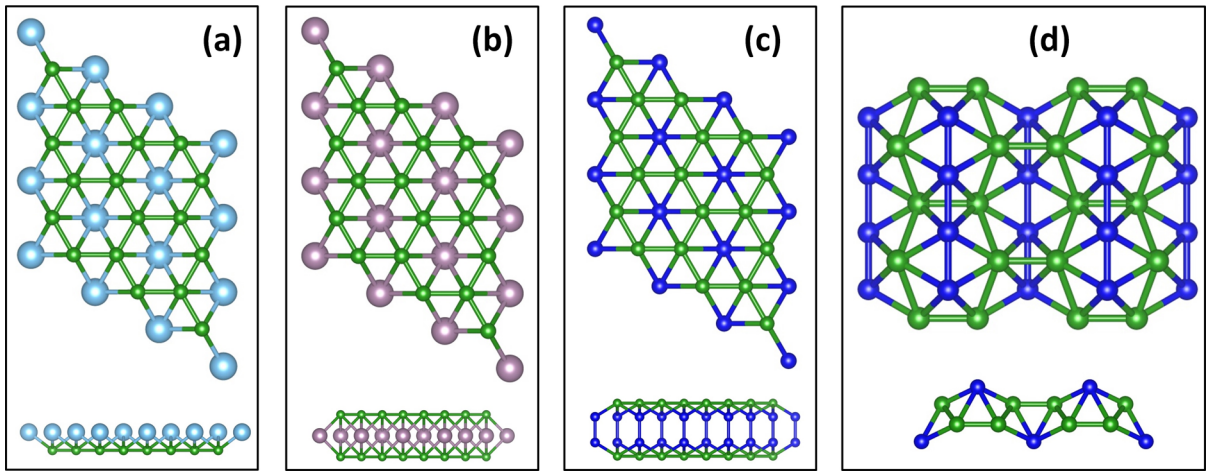

Figure 1. Top and side view of structures of (a) graphene-like monolayer boron sheet with divalent ions absorbed at hollow sites, (b) two graphene-like monolayer boron sheets with tetravalent ions in between, (c) *P6/mmm* boron bilayer predicted in ref 17, and (d) *Pmmn*-boron predicted in ref 18. Small green balls are boron atoms in hexagonal lattices, large light blue balls are divalent ions, large purple balls are tetravalent ions, and small blue balls are ionic-like boron atoms.

experimentally feasible if Dirac states can be realized in these nongraphene-like 2D boron sheets.

We notice that, among all the nongraphene-like boron sheets, some still preserve the honeycomb hexagonal lattice with the hollow sites (centers of the hexagon rings) being partially or fully filled with additional B atoms, like β_{12} (Figure 2a), α (Figure S1a), and δ_6 (Figure S1b) boron sheets.[19] Consequently, these sheets also have Dirac cones composed of the p_z electrons of the B atoms in the honeycomb hexagonal lattices, as seen in Figure 2b and Figure S1c,d, respectively. Due to the electron deficiency of B atoms compared to C atoms, the Dirac cones in boron sheets deviate from the Fermi levels. Additionally, those additional ionic-like B atoms can donate electrons to the honeycomb hexagonal lattices, leading to the additional shifts of Dirac cones. To realize these Dirac states, the Fermi levels need to cross the Dirac cones by filling or removing the electron states between the red and the green dashed lines in Figures 2b and S1c,d. Recently, Feng et al. have experimentally and theoretically determined β_{12} boron sheets grown on Ag(111) substrate as the first monolayer Dirac material beyond the honeycomb graphene-like structure,[26] thus demonstrating the feasibility of realizing Dirac states in non-graphene-like boron sheets. However, whether isolated 2D Dirac materials based on non-graphene-like boron sheets can stably exist, still remains unknown.

In this work, we show that, by rationally designing the nongraphene-like β_{12} boron sheets via the electron-accepting atoms like H, F, and Cl and the electron-donating atoms like Be, we identify several new isolated 2D Dirac materials β_{12}-$XBeB_5$ (X = H, F, Cl). Using β_{12}-$HBeB_5$ as an example, we carefully examine its stability to confirm that this newly designed Dirac material is energetically, dynamically, and thermally stable. Using the global search method for the lowest-energy structure, we further confirm β_{12}-$HBeB_5$ as the energy global minimum among its 2D allotropes. The robust stability of β_{12}-$HBeB_5$, combined with recent synthesis of β_{12} boron sheet, strongly indicates the experimental feasibility of this new 2D Dirac material. Our designed 2D Dirac material β_{12}-$HBeB_5$ has a high Fermi velocity of 0.73×10^6 m/s due to additional hopping through the ionic-like boron atoms, which is comparable to that of graphene. Additionally, we find that β_{12}-$HBeB_5$ can have very robust Dirac states against tensile strains, i.e., 12% biaxial tensile strain or 18% uniaxial tensile strain along the y direction, possibly an advantage for flexible electronic applications. Our work opens a new avenue to designing feasible 2D Dirac materials and stabilizing borophene sheets.

To shift the Fermi levels in these nongraphene-like boron sheets to Dirac cone positions, we follow two considerations. On one hand, the ionic-like boron atoms at the hollow sites can donate electrons to the hexagonal lattice. Because each hexagon ring only needs two electrons to form the Dirac state as discussed for the graphene-like 2D Dirac materials, one of the three electrons of the ionic-like boron atom thus should be taken away by electron-accepting atoms such as H, F, and Cl. On the other hand, for the hexagon ring without an additional boron atom at the center, two electrons need to be donated using a divalent atom such as Be. By considering the combination of the electron-accepting atoms and the electron-donating atoms, we investigate the feasibility of obtaining Dirac states in nongraphene-like born sheets that still preserve the honeycomb hexagonal lattices, including β_{12}, α, and δ_6 boron sheets. After careful check of the electronic properties and the stabilities, we find that functionalized α and δ_6 boron sheets do not have stable Dirac states (Figures S2 and S3 in the Supporting Information), and therefore we mainly focus on the design of Dirac states based on β_{12} boron sheets during the following discussions.

We perform our first-principles calculations using density-functional theory (DFT)[27,28] as implemented in the VASP code.[29,30] The global structure search in 2D space is performed using the IM2ODE package based on the differential evolution (DE) method.[31,32] Detailed calculation methods can be found in the Supporting Information.

The structure of our designed β_{12}-$HBeB_5$ monolayer is shown in Figure 2c, where a H atom serves to take one extra electron away from the ionic-like boron atom [$B^{(5)}$], while a Be atom donates two electrons to the empty hexagonal boron ring. The electron accepting and donating atoms can be attached to the same side or two sides of the β_{12} boron sheet. Our calculations show that the system with the electron-accepting and the electron-donating atoms on opposite sides has a lower energy by 0.06 eV/atom than the case with electron accepting

DOI: 10.1021/acs.jpclett.7b02163
J. Phys. Chem. Lett. 2017, 8, 4594−4599

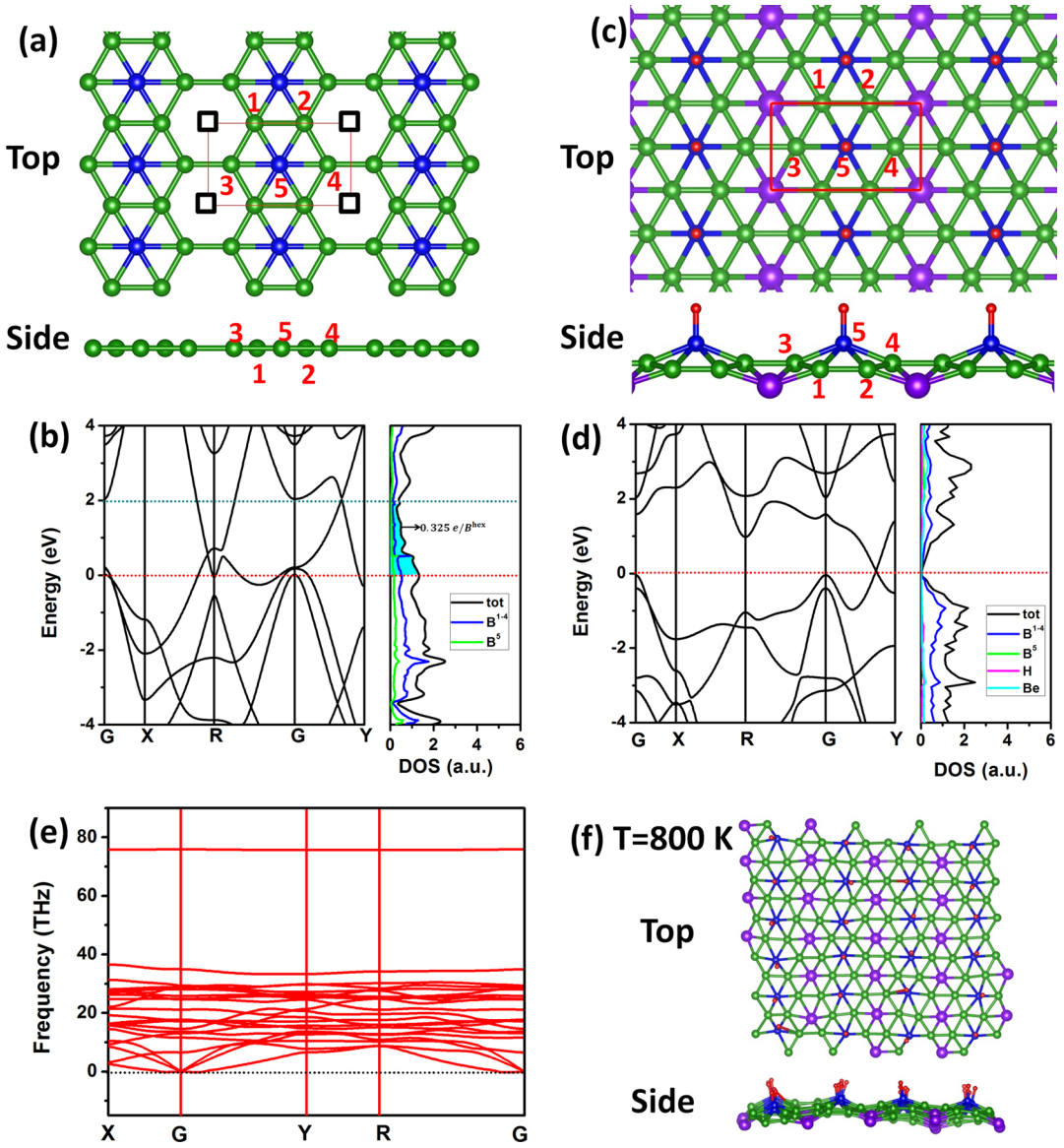

Figure 2. (a,c) Top and side view of structures of β_{12} boron sheet and β_{12}-$HBeB_5$. Small green balls are boron atoms in hexagonal lattices, small blue balls are ionic-like boron atoms, large purple balls are Be atoms, and small red balls are H atoms. Empty squares denote empty hollow sites. (b,d) Band structures and atomic projected density of states of β_{12} boron sheet and β_{12}-$HBeB_5$. Red dashed lines denote Fermi level positions and green dashed line denotes Dirac cone position in β_{12} boron sheet. The electronic states between the Fermi level and Dirac cone in the β_{12} boron sheet are highlighted in cyan color. (e) Phonon spectrum of β_{12}-$HBeB_5$ and (f) top and side view of 4 × 6 supercell of β_{12}-$HBeB_5$ after AIMD simulation at T = 800 K.

and donating atoms on the same side (Figure S4). We further confirm the structure of β_{12}-$HBeB_5$ by performing global structure search. We have performed a DE search at least two times with different sizes of $HBeB_5$ cells up to 21 atoms. It shows that β_{12}-$HBeB_5$ is the global energy minimum among its allotropes in the 2D space.

Due to the interactions between the attached atoms and boron atoms, all five boron atoms in β_{12}-$HBeB_5$ do not lie in the same plane as they are in the β_{12} boron sheet. Instead, $B^{(5)}$ is pulled up by the electron-accepting atom, and the hexagonal boron ring gets buckled, as seen in Figure 2c with atomic positions provided in the Supporting Information. The β_{12}-$HBeB_5$ sheet has a cohesive energy of 5.26 eV/atom. The total binding energy between β_{12} boron sheet, H atom and Be atom is 6.99 eV according to our calculations. Such large cohesive and binding energies indicate that β_{12}-$HBeB_5$ is strongly energetically stable. Phonon spectrum calculation shows that β_{12}-$HBeB_5$ is dynamically stable, without imaginary frequencies (Figure 2e). We further perform Ab-initio Molecular Dynamic simulation for β_{12}-$HBeB_5$ using a 4 × 6 supercell at a temperature of T = 800 K. After a running time of 10 ps, the structure of β_{12}-$HBeB_5$ is still well kept, as seen in Figure 2f, suggesting that β_{12}-$HBeB_5$ is also thermally stable at high temperatures. The robust stability of β_{12}-$HBeB_5$ combined with the earlier reported synthesis of β_{12} boron sheet strongly indicates the experimental feasibility of this new 2D Dirac material.

To further understand the stability of β_{12}-$HBeB_5$, we analyze the chemical bonding between atoms by calculating the electron localization function (ELF).[33] In Figure 3, the ELF isosurface at 0.75 shows that H atom indeed takes electrons from the $B^{(5)}$ atom, and the Be atom donates electrons to the

DOI: 10.1021/acs.jpclett.7b02163
J. Phys. Chem. Lett. 2017, 8, 4594−4599

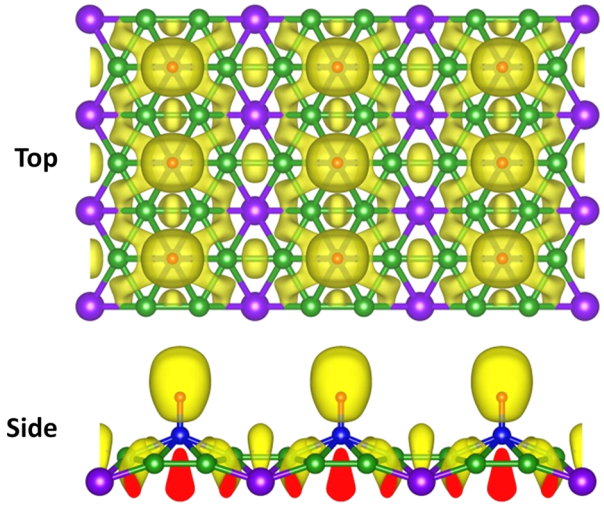

Figure 3. Top and side view of ELF in β_{12}-$HBeB_5$ with an isosurface of 0.75.

buckled hexagonal boron rings, in agreement with our intuitive design principles. Additionally, the H−$B^{(5)}$ and Be atoms are actually not completely ionized. Instead, a small amount of electrons lie between them and other boron atoms, indicating the weak covalent bonding. For example, the $B^{(5)}$ atom is weakly bonded to $B^{(3)}$ and $B^{(4)}$ atoms in the same primitive cells, and the Be atom is weakly bonded to $B^{(1)}$ and $B^{(2)}$ atoms in different primitive cells. The hexagonal-ring boron atoms form strong covalent bonds with a large amount of electrons in between. The overall bonding in β_{12}-$HBeB_5$ mimics carbon bonding in graphene, thus stabilizing this structure.

The calculated band structure of β_{12}-$HBeB_5$ is shown in Figure 2d. Due to the combined effects of the electron accepting and donating atoms, the Dirac bands in β_{12} boron sheet are shifted, and the Fermi level crosses no other bands but exactly the Dirac point, which is around (0, 1/3) in the reciprocal space, forming a Dirac state. We also sample the whole first Brillouin zone and confirm the Dirac state, as shown in Figure 4a. Spin−orbital coupling effect is checked, and no band gap opening is observed (Figure S5).

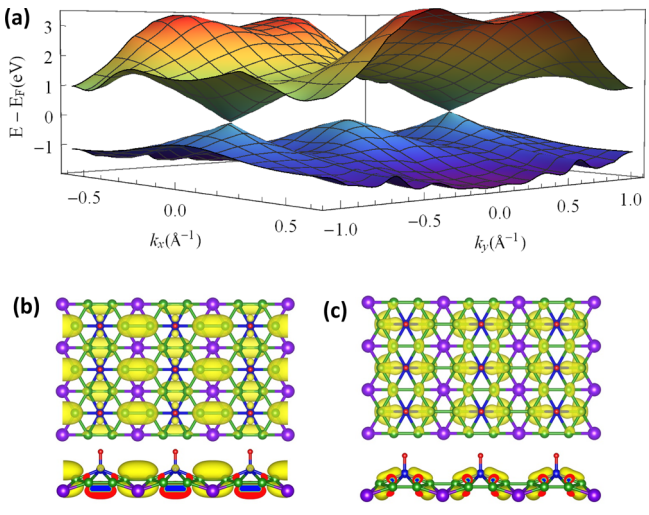

Figure 4. (a) 3D-plot of band structure of β_{12}-$HBeB_5$ in the first Brillouin zone. (b,c) Top and side view of VBM and CBM partial charge densities of β_{12}-$HBeB_5$.

To understand the origin of the Dirac state in β_{12}-$HBeB_5$, we plot the partial charge densities for the valence band maximum (VBM) and the conduction band minimum (CBM) at the Dirac point. As a mimic of graphene, β_{12}-$HBeB_5$ shows similar electronic characters around the Dirac point, i.e., both the VBM and the CBM mainly correspond to p_z orbitals from the hexagonal boron rings. However, due to the buckling in β_{12}-$HBeB_5$, the Dirac state also have some p_y orbitals for the VBM and some p_x orbitals for the CBM from $B^{(5)}$ atom, as shown in Figure 4b,c. We further confirm the electronic characters of the Dirac states in β_{12}-$HBeB_5$ by plotting the orbital-projected band structure (Figure S6).

It is interesting to note that, due to the existence of $B^{(5)}$, electron hopping among the boron atoms in the hexagonal rings can be strengthened, which could lead to a high Fermi velocity near the Dirac cone. Our calculation shows that the Fermi velocity in β_{12}-$HBeB_5$ can reach 0.73×10^6 m/s, which is comparable to that of graphene (0.82×10^6 m/s).[34] Using maximally localized Wannier function methods,[35] we derive the electron hopping parameters between atomic orbitals (Table S1). In graphene, it is known that Fermi velocity is derived as $v_F = \frac{3}{2}at$ from nearest neighbor hopping approximation,[8] where a is the nearest carbon−carbon distance, and t is the hopping parameter. Here in β_{12}-$HBeB_5$, the hexagonal lattice becomes distorted, and accurate derivation of the Fermi velocity from tight binding models is difficult. Nevertheless, we can still get Fermi velocity by averaging the results through all the nearest neighbor bonds, i.e.,$v_F = \frac{1}{12}\sum_{i=1}^{12}\frac{3}{2}a_i t_i$. Using our calculated hopping parameters and the atomic distances, we get a Fermi velocity of 0.79×10^6 m/s, in good agreement with our result from direct first-principles calculations. Note that, in graphene, the Fermi velocity decreases when graphene lattice is stretched, and Fermi velocity is dropped by more than 40% when the lattice is expanded by 20%.[36] In β_{12}-$HBeB_5$, while the average B−B distance in the hexagonal boron ring is about 20% larger than the C−C distance in graphene, the Fermi velocity is only 10% smaller due to the increased hopping parameters in β_{12}-$HBeB_5$ from additional hopping contributions through $B^{(5)}$ atom. This idea might be used while engineering Dirac materials to increase their Fermi velocities.

We note that, the eigen-energy of the highest occupied state at Γ point is about 0.1 eV smaller than that at the Dirac cone position. As a result, the robustness of the Dirac state against strain needs to be examined. We consider both biaxial and uniaxial strain effect on the Dirac state of β_{12}-$HBeB_5$. Figure 5 shows that the Dirac state is sustained under the biaxial strain between −0.5% and 12% (Figure 5a,b), or under the uniaxial strain between −5% and 12% along the x direction (Figure 5c,d), or under the uniaxial strain between −1% and 18% along y direction (Figure 5e,f). Larger compressive or tensile strain will make β_{12}-$HBeB_5$ metallic, either due to the increase of the eigen-energy of the highest occupied state at Γ point or due to the decrease of the eigen-energy of the lowest unoccupied state at R and Γ points. We find that the highest occupied state at the Γ point mainly has p_y character of $B^{(1)\text{-}(4)}$ atoms. Consequently, small compressive strain will easily push this state up to be higher than the state at the Dirac cone, resulting in the semimetal-to-metal transition. With this point in mind, we further check the Dirac state of β_{12}-$HBeB_5$ using the pseudopotential of local density approximation (LDA) functional, which yields lattice constants of about 1% ∼ 2% smaller than the PBE results. Nevertheless, our calculation shows that,

DOI: 10.1021/acs.jpclett.7b02163
J. Phys. Chem. Lett. 2017, 8, 4594−4599

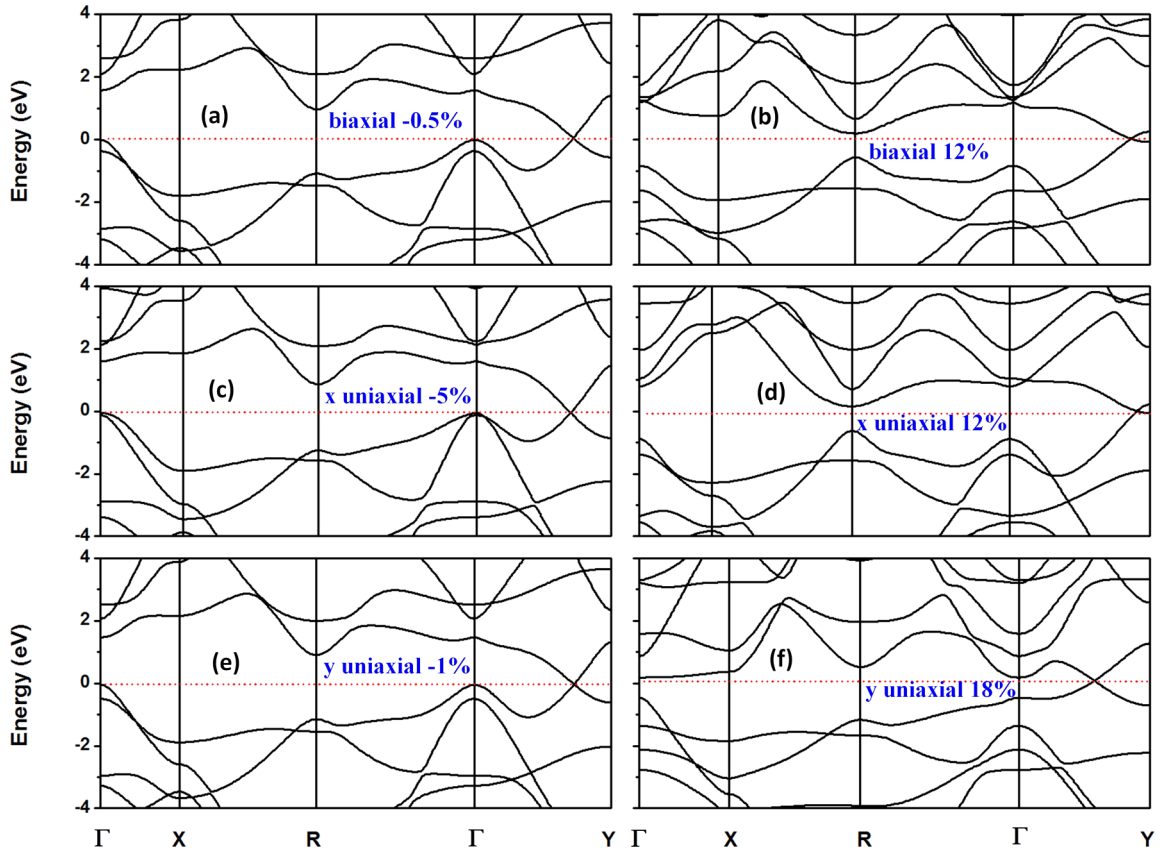

Figure 5. Band structure of β_{12}-$HBeB_5$ under (a,b) biaxial, (c,d) *x* uniaxial, and (e,f) *y* uniaxial strain.

the existence of Dirac state is independent of the selected functionals (see LDA band structure of β_{12}-$HBeB_5$ in the Supporting Information). Different from the highest occupied state at the Γ point, the lowest unoccupied state at te R or Γ point mainly corresponds to p_z characters. The tensile strain, which can largely push down the highest occupied state at the Γ point, slowly decreases the eigen-energy of the lowest unoccupied state at the R or Γ point. Consequently, the Dirac state of β_{12}-$HBeB_5$ can sustain extraordinary large tensile strain, i.e., the 12% biaxial and 18% uniaxial tensile strain, which might be a promising property of β_{12}-$HBeB_5$ for flexible electronic applications.

In summary, we show that, by rationally designing the nongraphene-like β_{12} boron sheets, we identify new isolated 2D Dirac materials β_{12}-$XBeB_5$ (X = H, F, Cl). Using β_{12}-$HBeB_5$ as an example, we demonstrate that β_{12}-$HBeB_5$ has very robust stability. Based on the recently reported successful synthesis of β_{12} boron sheets, we expect the experimental feasibility of this new 2D Dirac material as well. Our designed β_{12}-$HBeB_5$ not only has a high Fermi velocity of 0.73×10^6 m/s due to additional hopping through the ionic-like boron atoms, but also has very robust Dirac state against extraordinary large tensile strains, thus advantaging it for flexible electronic applications. Our designed β_{12}-$FBeB_5$ and β_{12}-$ClBeB_5$ show similar properties (Supporting Information). This work thus opens an avenue to designing feasible 2D Dirac materials and stabilizing borophene sheets. We note that the recently proposed Dirac boron hydride sheet with *Pbcm* symmetry[37] agrees with our design principles.

■ ASSOCIATED CONTENT

Supporting Information

The Supporting Information is available free of charge on the ACS Publications website at DOI: 10.1021/acs.jpclett.7b02163.

Calculation methods, structures, and band structures of α and δ_6 boron sheets; structures, band structures, and stabilities of functionalized α and δ_6 boron sheets; atomic position information on β_{12}-$HBeB_5$,; spin−orbital coupling and LDA band structure of β_{12}-$HBeB_5$; band structures of β_{12}-$FBeB_5$ and β_{12}-$ClBeB_5$ (PDF)

■ AUTHOR INFORMATION

Corresponding Authors

*E-mail: sxdu@iphy.ac.cn.
*E-mail: biy@rice.edu.

ORCID

Ji-Hui Yang: 0000-0003-0642-5344
Shixuan Du: 0000-0001-9323-1307
Hong-Jun Gao: 0000-0002-6766-0623

Author Contributions

§These two authors contribute equally to this work.

Notes

The authors declare no competing financial interest.

■ ACKNOWLEDGMENTS

Work at Rice was supported by the U.S. Army Research Office Grant W911NF-16-1-0255 and the Office of Naval Research Grant N00014-15-1-2372. The calculations were done on the Rice DAVinCI supercomputer. Work at the Institute of Physics,

DOI: 10.1021/acs.jpclett.7b02163
J. Phys. Chem. Lett. 2017, 8, 4594−4599

CAS, was supported by the National Key Research & Development Projects of China (2016YFA0202300) and NSFC (Nos. 61390501 and 51325204).

REFERENCES

(1) Mak, K. F.; Lee, C.; Hone, J.; Shan, J.; Heinz, T. F. Atomically Thin MoS_2: A New Direct-Gap Semiconductor. *Phys. Rev. Lett.* **2010**, *105*, 136805.
(2) Li, L.; Yu, Y.; Ye, G. J.; Ge, Q.; Ou, X.; Wu, H.; Feng, D.; Chen, X. H.; Zhang, Y. Black Phosphorus Field-effect Transistors. *Nat. Nanotechnol.* **2014**, *9*, 372−377.
(3) Naguib, M.; Mochalin, V. N.; Barsoum, M. W.; Gogotsi, Y. 25th Anniversary Article: MXenes: A New Family of Two-Dimensional Materials. *Adv. Mater.* **2014**, *26*, 992−1005.
(4) Mannix, A. J.; Zhou, X.-F.; Kiraly, B.; Wood, J. D.; Alducin, D.; Myers, B. D.; Liu, X.; Fisher, B. L.; Santiago, U.; Guest, J. R.; et al. Synthesis of Borophenes: Anisotropic, Two-dimensional Boron Polymorphs. *Science* **2015**, *350*, 1513−1516.
(5) Feng, B.; Zhang, J.; Zhong, Q.; Li, W.; Li, S.; Li, H.; Cheng, P.; Meng, S.; Chen, L.; Wu, K. Experimental Realization of Two-dimensional Boron Sheets. *Nat. Chem.* **2016**, *8*, 563−568.
(6) Zhang, Z.; Penev, E. S.; Yakobson, B. I. Two-dimensional Materials: Polyphony in B Flat. *Nat. Chem.* **2016**, *8*, 525−527.
(7) Wehling, T. O.; Black-Schaffer, A. M.; Balatsky, A. V. Dirac Materials. *Adv. Phys.* **2014**, *63*, 1−76.
(8) Castro Neto, A. H.; Guinea, F.; Peres, N. M. R.; Novoselov, K. S.; Geim, A. K. The Electronic Properties of Graphene. *Rev. Mod. Phys.* **2009**, *81*, 109−162.
(9) Bliokh, Y. P.; Freilikher, V.; Nori, F. Ballistic Charge Transport in Graphene and Light Propagation in Periodic Dielectric Structures with Metamaterials: A Comparative Study. *Phys. Rev. B: Condens. Matter Mater. Phys.* **2013**, *87*, 245134.
(10) Novoselov, K. S.; Geim, A. K.; Morozov, S. V.; Jiang, D.; Katsnelson, M. I.; Grigorieva, I. V.; Dubonos, S. V.; Firsov, A. A. Two-dimensional Gas of Massless Dirac Fermions in Graphene. *Nature* **2005**, *438*, 197−200.
(11) Zhang, Y.; Tan, Y. W.; Stormer, H. L.; Kim, P. Experimental Observation of the Quantum Hall effect and Berry's Phase in Graphene. *Nature* **2005**, *438*, 201−204.
(12) Wang, J.; Deng, S.; Liu, Z.; Liu, Z. The Rare Two-Dimensional Materials with Dirac Cones. *Natl. Sci. Rev.* **2015**, *2*, 22−39.
(13) Xu, L.-C.; Wang, R.-Z.; Miao, M.-S.; Wei, X.-L.; Chen, Y.-P.; Yan, H.; Lau, W.-M.; Liu, L.-M.; Ma, Y.-M. Two Dimensional Dirac Carbon Allotropes from Graphene. *Nanoscale* **2014**, *6*, 1113−1118.
(14) Zhang, H.; Li, Y.; Hou, J.; Du, A.; Chen, Z. Dirac State in the FeB_2 Monolayer with Graphene-Like Boron Sheet. *Nano Lett.* **2016**, *16*, 6124−6129.
(15) Zhang, L. Z.; Wang, Z. F.; Du, S. X.; Gao, H.-J.; Liu, F. Prediction of a Dirac State in Monolayer TiB_2. *Phys. Rev. B: Condens. Matter Mater. Phys.* **2014**, *90*, 161402.
(16) Mu, Y.; Ding, F.; Lu, H. Strain-induced Metal-semimetal Transition of BeB_2 Monolayer. *RSC Adv.* **2015**, *5*, 11392−11396.
(17) Xie, S.-Y.; Li, X.-B.; Tian, W. Q.; Chen, N.-K.; Zhang, X.-L.; Wang, Y.; Zhang, S.; Sun, H.-B. First-principles Calculations of a Robust Two-dimensional Boron Honeycomb Sandwiching a Triangular Molybdenum Layer. *Phys. Rev. B: Condens. Matter Mater. Phys.* **2014**, *90*, 035447.
(18) Ma, F.; Jiao, Y.; Gao, G.; Gu, Y.; Bilic, A.; Chen, Z.; Du, A. Graphene-like Two-Dimensional Ionic Boron with Double Dirac Cones at Ambient Condition. *Nano Lett.* **2016**, *16*, 3022−3028.
(19) Zhou, X.-F.; Dong, X.; Oganov, A. R.; Zhu, Q.; Tian, Y.; Wang, H.-T. Semimetallic Two-Dimensional Boron Allotrope with Massless Dirac Fermions. *Phys. Rev. Lett.* **2014**, *112*, 085502.
(20) Cheng, T.; Lang, H.; Li, Z.; Liu, Z.; Liu, Z. Anisotropic Carrier Mobility in Two-Dimensional Materials with Tilted Dirac Cones: Theory and Application. *Phys. Chem. Chem. Phys.* **2017**, DOI: 10.1039/C7CP03736H.
(21) Wu, X.; Dai, J.; Zhao, Y.; Zhuo, Z.; Yang, J.; Zeng, X. C. Two-Dimensional Boron Monolayer Sheets. *ACS Nano* **2012**, *6*, 7443−7453.
(22) Penev, E. S.; Bhowmick, S.; Sadrzadeh, A.; Yakobson, B. I. Polymorphism of Two-Dimensional Boron. *Nano Lett.* **2012**, *12*, 2441−2445.
(23) Liu, Y.; Penev, E. S.; Yakobson, B. I. Probing the Synthesis of Two-Dimensional Boron by First-Principles Computations. *Angew. Chem., Int. Ed.* **2013**, *52*, 3156−3159.
(24) Zhang, Z.; Yang, Y.; Gao, G.; Yakobson, B. I. Two-Dimensional Boron Monolayers Mediated by Metal Substrates. *Angew. Chem., Int. Ed.* **2015**, *54*, 13022−13026.
(25) Zhou, X.-F.; Oganov, A. R.; Wang, Z.; Popov, I. A.; Boldyrev, A. I.; Wang, H.-T. Two-Dimensional Magnetic Boron. *Phys. Rev. B: Condens. Matter Mater. Phys.* **2016**, *93*, 085406.
(26) Feng, B.; Sugino, O.; Liu, R.-Y.; Zhang, J.; Yukawa, R.; Kawamura, M.; Iimori, T.; Kim, H.; Hasegawa, Y.; Li, H.; et al. Dirac Fermions in Borophene. *Phys. Rev. Lett.* **2017**, *118*, 096401.
(27) Hohenberg, P.; Kohn, W. Inhomogeneous Electron Gas. *Phys. Rev.* **1964**, *136*, B864−B871.
(28) Kohn, W.; Sham, L. J. Self-Consistent Equations Including Exchange and Correlation Effects. *Phys. Rev.* **1965**, *140*, A1133−A1138.
(29) Kresse, G.; Furthmüller, J. Efficient Iterative Schemes for *ab initio* Total-energy Calculations Using a Plane-wave Basis Set. *Phys. Rev. B: Condens. Matter Mater. Phys.* **1996**, *54*, 11169−11186.
(30) Kresse, G.; Furthmüller, J. Efficiency of ab-initio Total Energy Calculations for Metals and Semiconductors Using a Plane-Wave Basis Set. *Comput. Mater. Sci.* **1996**, *6*, 15−50.
(31) Zhang, Y.-Y.; Gao, W.; Chen, S.; Xiang, H.; Gong, X.-G. Inverse Design of Materials by Multi-objective Differential Evolution. *Comput. Mater. Sci.* **2015**, *98*, 51−55.
(32) Chen, H.-Z.; Zhang, Y.-Y.; Gong, X.; Xiang, H. Predicting New TiO_2 Phases with Low Band Gaps by a Multiobjective Global Optimization Approach. *J. Phys. Chem. C* **2014**, *118*, 2333−2337.
(33) Savin, A.; Nesper, R.; Wengert, S.; Fässler, T. F. ELF: The Electron Localization Function. *Angew. Chem., Int. Ed. Engl.* **1997**, *36*, 1808−1832.
(34) Malko, D.; Neiss, C.; Viñes, F.; Görling, A. Competition for Graphene: Graphynes with Direction-Dependent Dirac Cones. *Phys. Rev. Lett.* **2012**, *108*, 086804.
(35) Mostofi, A. A.; Yates, J. R.; Lee, Y.-S.; Souza, I.; Vanderbilt, D.; Marzari, N. Wannier90: A tool for Obtaining Maximally-localised Wannier Functions. *Comput. Phys. Commun.* **2008**, *178*, 685−699.
(36) Wong, J.-H.; Wu, B.-R.; Lin, M.-F. Strain Effect on the Electronic Properties of Single Layer and Bilayer Graphene. *J. Phys. Chem. C* **2012**, *116*, 8271−8277.
(37) Jiao, Y.; Ma, F.; Bell, J.; Bilic, A.; Du, A. Two-Dimensional Boron Hydride Sheets: High Stability, Massless Dirac Fermions, and Excellent Mechanical Properties. *Angew. Chem., Int. Ed.* **2016**, *55*, 10292−10295.

DOI: 10.1021/acs.jpclett.7b02163
J. Phys. Chem. Lett. 2017, 8, 4594−4599